

In Situ Preparation, Electrospinning, and Characterization of Polyacrylonitrile Nanofibers Containing Silver Nanoparticles

G.Naddaf Sichani,¹ M. Morshed,¹ M. Amirasr,² D. Abedi³

¹Department of Textile Engineering, Isfahan University of Technology, Isfahan, Iran

²Department of Chemistry, Isfahan University of Technology, Isfahan, Iran

³Department of Pharmaceutical Biotechnology and Isfahan Pharmaceutical Sciences Research Center, School of Pharmacy, Isfahan University of Medical Sciences, Isfahan 81745-359, Iran

Received 3 July 2008; accepted 17 September 2009

DOI 10.1002/app.31436

Published online 17 December 2009 in Wiley InterScience (www.interscience.wiley.com).

ABSTRACT: Silver nanoparticles were prepared from a polyacrylonitrile (PAN)/*N,N*-dimethylformamide solution of silver nitrate (0.05–0.5 wt %) with light treatment (xenon arc) to reduce Ag⁺ ions into Ag⁰. The formation of silver nanoparticles in the PAN solution and the effect of treatment time on the numbers of silver nanoparticles, their average diameter and size distribution were investigated by UV–visible spectroscopy. In addition, the average size of silver nanoparticles and their shapes in colloidal solution were determined by transmission electron microscopy images and found to be on the order of 10 nm. The resulting solution was electrospun into PAN nanofibers.

An increase in the salt concentration led to decreases in the nanofiber diameter and bead numbers (determined by scanning electron microscopy images) and an increase in the crystallinity (confirmed by X-ray diffraction patterns). A continuous rate of silver release from the nanofiber web was monitored by the atomic absorption technique. These nanofibers showed strong antibacterial activity against *Pseudomonas aeruginosa*. © 2009 Wiley Periodicals, Inc. *J Appl Polym Sci* 116: 1021–1029, 2010

Key words: colloids; electron microscopy; nanotechnology; polyolefins; synthesis

INTRODUCTION

Nowadays, the preparation of nanofibers containing metal nanoparticles, especially silver nanoparticles, has drawn great attention^{1–6} because of the fact that these nanocomposites combine the remarkable properties of metal nanoparticles with the outstanding characteristics of polymeric nanofibers.¹ Nanofibers themselves, because of their high surface area, have different applications in composites, filtration,^{7,8} protective textiles,^{8,9} medical applications, the biomedical sciences,⁹ and so on. With the addition of nanosilver, nanofibers will be given other properties, such as catalytic,¹⁰ optical,¹ and especially antibacterial properties.^{3,11,12} This is due to the fact that silver nanoparticles are strong antibacterial agents that can kill different bacteria,¹³ and with just a small amounts of silver precursor, large surface areas that have antibacterial properties can be obtained.¹⁴ Lately, the application of antibacterial synthetic [polyacrylonitrile (PAN) and poly(vinyl chloride) (PVC)] nanofibers for air filtration has been reported.¹⁵

There are different methods of preparing a polymeric matrix containing metal nanoparticles. The mechanical mixing of a polymer solution and nanoparticles powder is an easy method,¹⁶ with the disadvantage that it undergoes agglomeration.^{16,17} Because of this disadvantage, recent methods based on the *in situ* reduction of metal ions^{18–21} and the *in situ* polymerization of monomers²² have attracted more attention. The *in situ* reduction method is based on the reduction of silver ions, provided by a metal salt, into Ag⁰ in a polymeric matrix.

Different polymers, such as poly(*N*-vinylpyrrolidone),⁴ cellulose acetate,³ polypyrrole,²³ PAN,^{1,2,4,22} polyurethane,¹⁷ poly(vinyl alcohol) (PVA),¹¹ and polyacrylamide,²⁴ have been used as stabilizers for silver nanoparticles. It was reported that the narrowest size distribution characteristics were obtained with poly(ethylene imine).¹⁸

Depending on the reduction time, equipment, type of polymer, and end uses, different methods can be used for *in situ* reduction. Ag⁺ ions can be reduced to silver nanoparticles with chemicals (e.g., an aqueous solution of N₂H₅OH, potassium borohydride),^{25–29} radiation (e.g., UV radiation,^{19,27} γ rays,^{27,30} sunlight²), and high temperatures.⁵

Yang et al.² in 2003 were the first to report the *in situ* preparation of nanosilvers in a PAN/*N,N*-dimethylformamide (DMF) solution. They reduced silver

Correspondence to: M. Morshed (morshed@cc.iut.ac.ir).

ions in the PAN/DMF solution by hydrazine hydroxide. The silver nanoparticles with a polymeric cover were then precipitated by the addition of acetone. The precipitate were separated and redissolved in DMF and electrospun into PAN/Ag nanofibers. Their production process was time-consuming (four steps and 36 h for the mixing solution), and their nanofiber production process was tedious because of the large size of the silver nanoparticles (100 nm), and it led to some precipitation during the electrospinning process.

Wang et al.¹ in 2005 omitted the precipitation stage with acetone. They electrospun a PAN/DMF solution that contained silver ions into nanofibers and then reduced the silver ions on the nanofibers by hydrazine hydroxide. Their process was shorter and easier (three steps and 24 h of mixing), but because of presence of a high concentration of silver nitrate (437% on the basis of the polymer weight) in the electrospinning solution, this procedure may lead to inhomogeneity in the distribution of silver nanoparticles in the produced nanofibers. In addition, we showed that good antibacterial properties can be achieved with a very low concentration of silver ions.

Youk et al.⁴ in 2005 also prepared Ag nanoparticles *in situ* in a PAN/DMF solution by using just DMF as the reducing agent. Their process was easy (two steps) but long (10 days).

Although PAN nanofibers containing silver nanoparticles have been prepared by the aforementioned workers,^{1,2,4} to the best of our knowledge, no quantitative analysis of the properties, such as the antibacterial activity, yellowness index (YI), silver-ion release, and X-ray diffraction (XRD), of their prepared PAN/Ag nanofibers have yet been reported.

In this study, the *in situ* preparation of silver nanoparticles in a PAN/DMF solution was carried out over 4 h for the first time with a xenon arc lamp (a lamp that closely mimics natural daylight), and the resulting colloidal solution was then electrospun into nanofibers. Moreover, different methods, such as ultraviolet-visible (UV-vis) spectroscopy, XRD, reflectance spectroscopy, and transmission and scanning electron microscopy (SEM) techniques, were used to characterize the PAN nanofibers and silver nanoparticles. Also, the silver release of the prepared PAN nanofibers containing silver nanoparticles and their antibacterial features against *Escherichia coli*, *Staphylococcus aureus*, and *Pseudomonas aeruginosa* were investigated.

EXPERIMENTAL

Materials

PAN (weight-average molecular weight = 100,000 and number-average molecular weight = 70,000) was provided by Polyacryl Co. (Isfahan, Iran). AgNO₃

(99.99%) and (DMF) were purchased from Sigma-Aldrich and were used as received. Gram-positive *S. aureus* PTCC 1112 bacteria and Gram-negative *E. coli* PTCC 1338 and *P. aeruginosa* PTCC 1074 bacteria were used (Persian Collection, Tehran, Iran). Nutrient agar, nutrient broth, and Normalin were also used.

Solution preparation

PAN was dissolved in DMF to make solutions with a concentration of 10 wt %, and 0.05–0.5 wt % AgNO₃ (the weight percentage of AgNO₃ in the solution was calculated on the basis of PAN weight) was then added to the solutions. The solutions containing silver salt were stirred for 24 h at 27°C. During the mixing process, the samples were covered with aluminum foil to prevent the probable and unwanted reduction of silver ions. Then, the solutions were exposed to light (a xenon arc) by a xenon tester 150 S for 4 h (irradiation was continued until the absorption spectrum no longer changed) to increase the rate of Ag⁺ reduction into Ag⁰. Yellow coloration of the PAN/DMF solution containing silver salt was observed with the naked eye after the first 15 min of irradiation; this confirmed the reduction of silver ions and the subsequent formation of silver atoms.⁴ To monitor the changes in the colloidal mixture, consecutive absorption spectra were obtained at various time intervals during the course of irradiation.

Electrospinning of the nanofibers

The apparatus for the electrospinning was assembled as reported elsewhere.^{1,2,4,31} A high-voltage power supply was used to generate an electric field of 0–20 kV. The polymer solution was loaded into a 1.0-mL syringe with a capillary tip having a 2.5-cm length and an outer diameter of 0.7 mm. The needle of the syringe was connected to the positive electrode by a copper wire. A flat piece of aluminum foil, which was connected to the negative electrode, was used to collect the nonwoven nanofiber mat. A syringe pump was used to control the constant mass flow of the polymer solution during the electrospinning. All of the spinning experiments were performed under ambient conditions. The electrospinning variables for the preparation of the nanofiber webs for different analyses are presented in Table I.

Characterization

UV-vis absorption spectroscopy of the PAN/DMF/Ag colloidal solutions from 300 to 800 nm were carried out on a UV-visible spectrophotometer (Cary UV-VIS 300, Variyan, PaloAlto, CA) at room temperature with a 1-cm quartz cell. To investigate the effect of the silver precursor (silver nitrate)

TABLE I
Electrospinning Variables and Conditions

Distance between the collector and needle tip (cm)	Electrospinning time (min)	Feeding rate (mL/h)	Voltage (kV)	Silver nitrate (wt %; polymer based)	PAN/DMF (wt %)	Analysis
15	3	0.15	10.1	0	10	SEM
15	0.15	0.15	10.1	0.05	10	SEM
15	0.15	0.15	10.1	0.5	10	SEM
20	3	0.1	13.13	0.5	10	TEM
15	930	0.6	15.65	0.5	13	XRD
15	630	0.6	14.74	0.2	13	Silver release
15	1200	0.6	17.1	0	13	YI
15	1200	0.6	17.1	0.05	13	YI
15	1200	0.6	17.1	0.2	13	YI
15	1200	0.6	17.1	0.5	13	YI

concentration on the electrospinning solution and electrospun nanofibers accordingly, the conductivity of the prepared silver colloidal solutions containing different amounts of silver precursor were determined by a conductometer (Konduktometer CG 855, Schott, Hofheim, Germany) at 25°C.

We obtained transmission electron microscopy (TEM) images with a transmission electron microscope (CEM 902 ZPICC, Jena, Germany) operating at 100 kV by placing one drop of the colloidal solution onto a carbon-coated grid and letting the drop dry. The morphology of the electrospun PAN/Ag gold-coated nanofibers was determined with SEM (Philips, XL-30, Eindhoven, Netherlands). The average diameters of the electrospun nanofibers and prepared nanoparticles were determined by analysis of the SEM and TEM images with Motic software (DC imaging, Chester, PA). The size distribution was derived from histograms. Fourier transform infrared (FTIR) spectroscopy of the PAN/DMF solutions containing silver nanoparticles was performed in transmission mode on KBr pellets with a BOMEM MB-series 100 FTIR spectrophotometer (Victoria, Australia). The XRD patterns were taken on a Philips X-ray diffractometer (model XPERT-MPD, Philips, Eindhoven, Netherlands). The YIs of the nanofiber webs (4 cm²) were determined by a reflectance spectrophotometer (Datacolor, TexFlash, Zurich, Switzerland) under standard conditions (27°C and 60% relative humidity). Ag⁺ ions extracted from the PAN/Ag electrospun web (weight = 0.1 g and area = 49 cm²) in deionized water with the pH adjusted to 4.5 with a HNO₃ solution at 37 ± 2°C (to simulate natural conditions) were measured by an atomic absorption spectroscope (SCHOTT 2380, PerkinElmer, USA).

It was reported³² that PAN fibers bound *S. aureus* and *P. aeruginosa* bacteria at high ratios (>80%), and consequently, the preparation of antibacterial PAN^{33,34} fibers has been discussed in many articles. The antibacterial activity of prepared PAN nanofiber webs (4 cm²) with and without silver nanoparticles

were tested against Gram-positive *S. aureus* (PTCC 1112), Gram-negative *E. coli* (PTCC 1338), and *P. aeruginosa* (PTCC 1074) according to AATCC test method 100-1999. Before inoculation of the bacteria, the pieces of the webs were disinfected by UV ($\lambda = 220$ nm) irradiation for 1 min.³⁵

RESULTS AND DISCUSSION

In situ preparation of the silver nanoparticles in the PAN/DMF solution

The nanometallic particles exhibited a high optical absorbance because of the discrete energy levels of electrons caused by the quantum size effect. The silver nanoparticles had a rather strong absorption band in the visible region (~410 nm). Although the exact position of the absorption maximum in the UV-vis spectra depended on the dielectric constant and the range and shape of the nanoparticles, the spectra gave preliminary information about the size and size distribution of the silver nanoparticles.¹⁰ In this study, UV-vis spectroscopy was used to determine the formation of metallic silver in the PAN/DMF solution and to record changes in the nanoparticle size, size distributions, and number of silver nanoparticles during their synthesis.^{3,18,30} Figure 1 shows drastic changes in the absorption spectrum of a 10 wt % PAN/DMF solution containing 0.2 wt % AgNO₃ in the course of irradiation. All of these spectra exhibited strong peaks centered at about 418 nm with a gradual increase in the intensity with irradiation time [Fig. 2(a)]. This increase was attributed to a significant increase in the amount of reduced silver.³⁶ Table II shows a summary of the different preparation parameters of the PAN/DMF solution containing silver nanoparticles. The rate of silver-ion reduction in the PAN/DMF solution by N₂H₅OH was more than that by the xenon arc but needed a precipitation process, as Yang reported.²

The maximum absorption shifted slightly to longer wavelengths during irradiation [Fig. 2(b)]; this

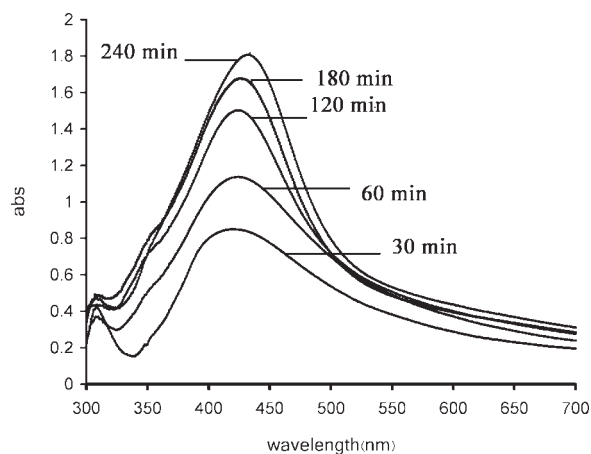


Figure 1 UV-vis spectra of 10 wt % PAN/DMF solution containing 0.2 wt % AgNO_3 in the course of 4 h of irradiation.

indicated that the size of the nanoparticles increased during this process.^{1,4,5,26}

Cluster size growth was carried out through different methods, as presented in eqs. (1)–(5).²⁹

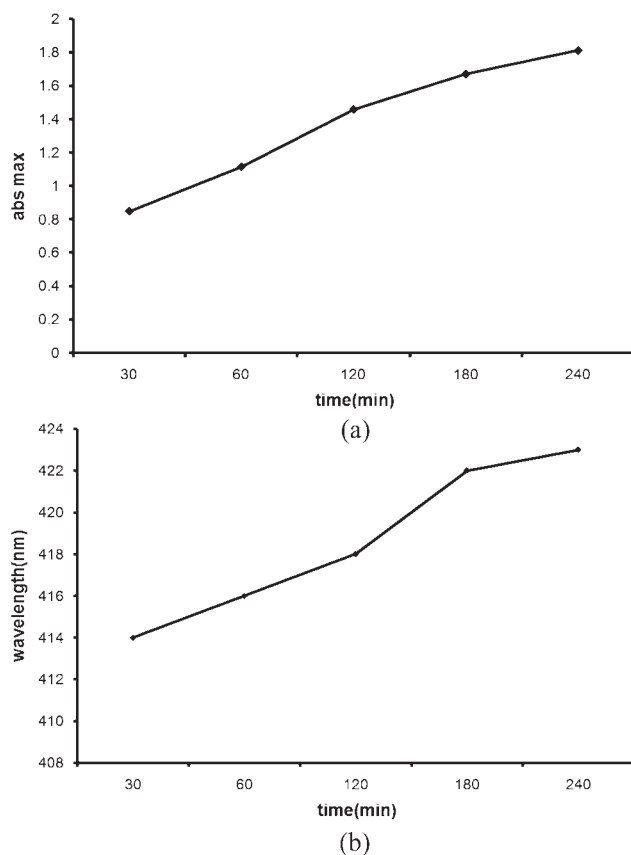
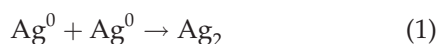
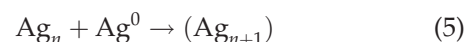
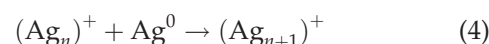
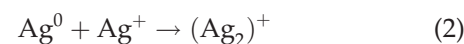


Figure 2 (a) Absorption maximum and (b) wavelength of the absorption maximum of a 10 wt % PAN/DMF solution containing 0.2 wt % AgNO_3 in the course of 4 h of irradiation versus irradiation time.



The position of the plasmon band of nanoparticles as a measure of the experimentally determined and theoretically calculated particle radii.²⁹ The peak with a maximum wavelength of about 420 nm indicated the presence of silver nanoparticles with sizes of about 10 nm and smaller.¹ In this study, according to the UV-vis spectra, nanoparticles with mean diameters of about 10 nm were prepared *in situ* after 4 h of irradiation. In the subsequent characterizations, the exact mean diameter of the nanoparticles was determined to be 10.2 nm by the TEM images.

It was evident that the full width at half-maximum of the UV-vis spectra (Fig. 1) decreased (from 163 to 124) with time, which, in turn, was an indication of the decrease in the nanoparticle size distribution.^{14,18,26} It has been well established that the size distribution of nanoparticles has a significant influence on prepared solution features, such as the solution stability.³⁷

Characterization of the silver nanoparticles in PAN/DMF

Figure 3 shows a typical TEM image of silver nanoparticles. Well-distributed spherical shaped silver nanoparticles with sizes ranging from 6 to 19 nm were observed. The nanoparticle size histogram showed a narrow size distribution around 10 nm for the silver nanoparticles. A high correlation between the nanoparticle size and UV-vis spectra was evident from these observations. It appeared that PAN played a significant role in stabilizing the silver nanoparticles. These results were comparable to those reported by Lee et al.⁴ and Wang et al.,¹ who claimed that averages of 5- and 10-nm silver

TABLE II
Summary of the Different Preparation Parameters of the PAN/DMF Solutions Containing Silver Nanoparticles

Reference	Silver nitrate concentration (wt % based on polymer weight)	PAN/DMF (wt %)	Reducing agent	Reduction process time (h)
Yang ²	64	0.01	$\text{N}_2\text{H}_5\text{OH}$	2
Youk ⁴	<0.5	7	DMF	240
This study	<0.5	10	DMF plus an arc xenon lamp	4

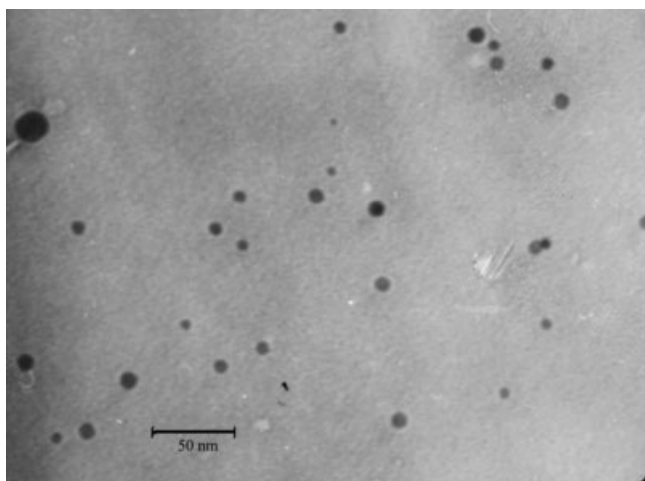


Figure 3 Typical TEM image of silver nanoparticles in a 10 wt % PAN/DMF solution containing 0.5 wt % AgNO_3 after 4 h of irradiation ($140,000\times$ magnitude).

nanoparticles were synthesized with DMF and $\text{N}_2\text{H}_5\text{OH}$ as the reducing agents, respectively.

FTIR spectra of the colloidal PAN/Ag solution

To investigate the effect of the addition of silver nitrate to the PAN/DMF solution, FTIR spectroscopy was used. Figure 4 shows the FTIR spectra of PAN/DMF solutions with and without silver nitrate. The positions of all peaks in the IR spectra of both the PAN/DMF and PAN/DMF/Ag solutions were almost identical. This means that there was no noticeable shift in the C—N triple-bond vibration (at 2234 cm^{-1}) by the addition of silver salt that could be detected by the IR measurements. Therefore, the possibility of the formation of coordination bonds between PAN and silver was negligible. These observations were in agreement with those reported by Zhang et al.²² However, the nitrile groups in the

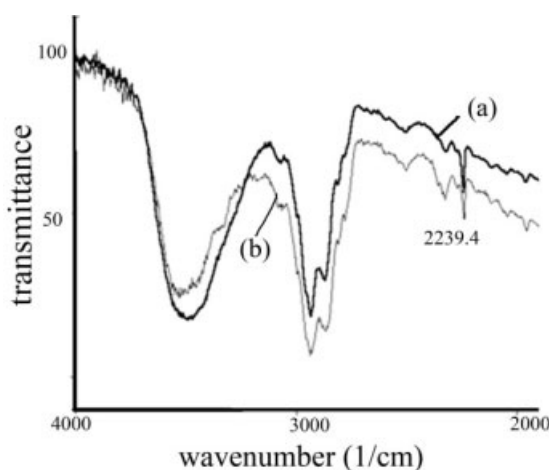
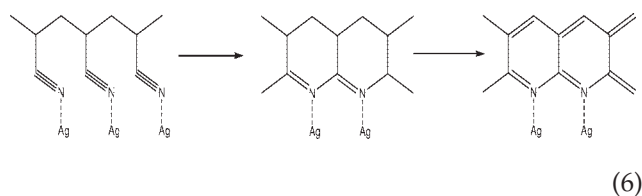


Figure 4 FTIR spectra of 10 wt % PAN/DMF solutions (a) without AgNO_3 and (b) with 0.5 wt % AgNO_3 .

PAN chains may have polymerized in the presence of silver ions [eq. (6)], and therefore, the number of C—N triple bonds decreased accordingly. This was confirmed by the reduction of the intensity of the IR peak corresponding to the nitrile group and was in agreement with the results obtained by Wang et al.¹ through the Raman scattering spectrum of the PAN/Ag nanocomposite:



Solution conductivity

In the electrospinning process, one of the parameters that had a significant effect on the properties of prepared nanofibers was the conductivity of the electrospinning solution. Therefore, the conductivities of the colloidal solutions containing different amounts of silver precursor were measured (Fig. 5).

Silver salt contents of 0.5 wt % and less ($<0.5\text{ wt %}$) caused a significant increase in the conductivity of the solution.

Morphology of the PAN nanofiber web

To investigate the effect of the addition of silver nitrate on the morphology and diameter of the nanofibers, SEM images were used. Figures 6 show SEM images of PAN nanofibers containing different amounts of silver nanoparticles. Silver salt contents of 0.5 wt % and less ($<0.5\text{ wt %}$) caused a significant decrease in the average nanofiber diameter (from 170.8 to 113.6 nm), as the SEM images and their histograms showed. The addition of salt led to an increase in the charge density in the ejected jet, and thus, stronger elongation forces were imposed on

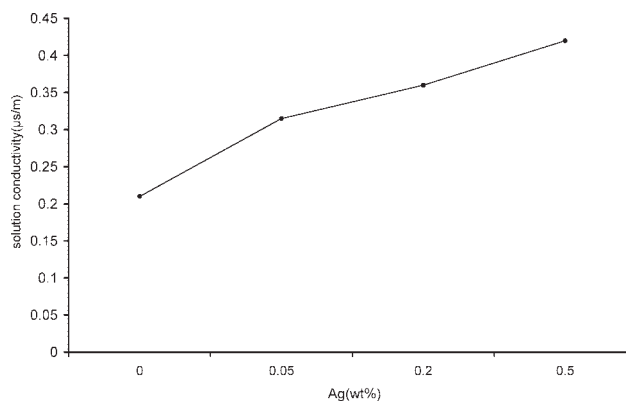


Figure 5 Changes in the conductivity of 10 wt % PAN/DMF colloidal solutions with different amounts of silver precursor.

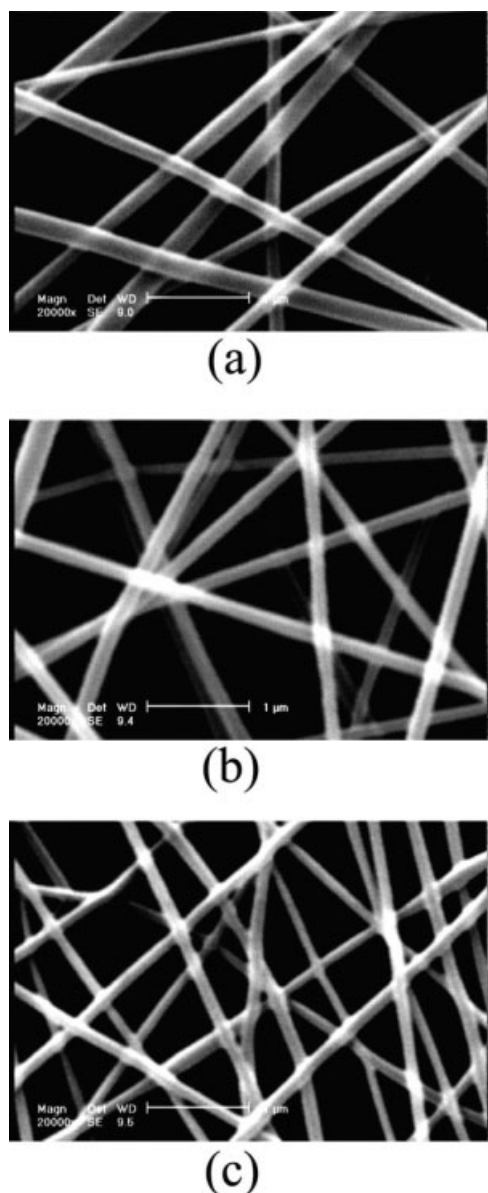


Figure 6 SEM images of the PAN nanofibers containing silver nanoparticles prepared from 10 wt % PAN/DMF solutions containing (a) 0.0, (b) 0.05, and (c) 0.5 wt % AgNO_3 .

the jets because of the self-repulsion of excess charges under the electrical field; this resulted in substantially finer nanofibers. These findings were in agreement with the results obtained by Wang et al.¹ and Lee et al.⁴

The effect of silver salt on the surface structure of the PAN nanofibers was also investigated. As shown in Figure 7, beads (the most important fault that occurred during the electrospinning of the nanofibers) changed from spherical to spindle-like shapes, and their numbers decreased as the amount of silver salt was increased from 0 to 0.5 wt %. This was due to the stronger elongation forces that were imposed on the jet during electrospinning in the presence of silver salt.

XRD pattern of the PAN/Ag nanofiber web

To study the presence of silver nanoparticles in the prepared nanofibers and investigate their crystal structure, X-ray analysis was used. The XRD patterns of acrylic nanofibers with and without silver nanoparticles are shown in Figure 8. The XRD pattern of the pure PAN nanofibers showed a sharp crystalline peak at a 2θ value of 24° and a broad noncrystalline peak at about $16\text{--}20^\circ$.²² In the XRD pattern of PAN nanofibers containing silver nanoparticles, four new additional peaks were observed that corresponded to the face-center cubic silver phase. These peaks appeared at 2θ values of 38.44 , 44.52 , 64.84 , and 78.15° , which corresponded to the (111), (200), (220), and (311) planes of silver, respectively. These values were close to those in the International Center for Diffraction Data (ICDD) card (card no.4-783). Moreover, the XRD patterns showed that the addition of silver nitrate to the electrospinning solution enhanced the crystallinity, presumably because of the formation of some cyclic structure in the PAN chains,³⁸ as mentioned in the FTIR section.

YI of the nanofiber web

One of the disadvantages of the use of silver nanoparticles as an antimicrobial agent is the tendency of the substrate to turn yellow.²⁵ To determine YI of the prepared nanofibers and investigate the effect of the storage time on their yellowness, UV reflectance spectroscopy was used. The results are shown in Figure 9. YI was calculated according to the following Bill Mayer equation:

$$\text{YI} = (125.50X - 105.842Z)/Y \quad (7)$$

where X , Y , and Z are the Commission Internationale de l'Éclairage tristimulus values. This equation was accepted by the American Society of Testing Materials (ASTM D 1925) for textiles, and it conforms to visual perception.³⁹

As shown in Figure 9, with increasing storage time, YI increased, presumably because of the gradual reduction of silver ions to metallic silver and the simultaneous oxidation of the PAN polymer, although there was a gradual decrease in the rate of changes.

Silver-ion release

The rate and the amount of silver release were the key factors in the antimicrobial performance of the nanofibers. It was reported that a steady and prolonged release of silver, with a concentration above 0.1 ppb, can inhibit the growth of bacteria.⁶ The results of silver release from the PAN/Ag nanofiber

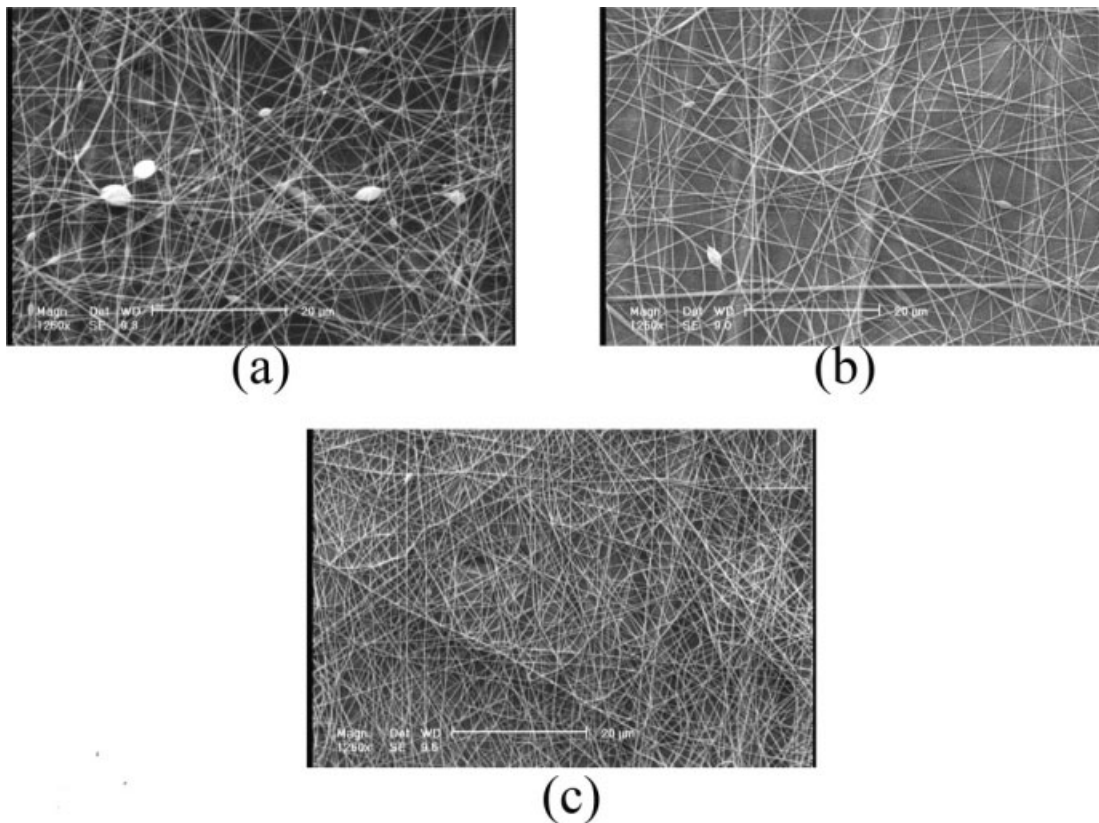


Figure 7 SEM images of PAN nanofibers prepared from 10 wt % PAN/DMF solutions (a) without AgNO₃ and with (b) 0.05 and (c) 0.5 wt % AgNO₃.

web, investigated by atomic absorption spectroscopy, are shown in Figure 10. It was evident that the release of Ag⁺ was relatively fast at the beginning and became slower and relatively steady along with the incubation time (140 h). Therefore, the PAN/Ag nanofiber web was expected to show antibacterial activity, as is demonstrated in the next section.

Antibacterial tests

The antibacterial activity of ultrafine PAN fibers with and without silver nanoparticles was examined against Gram-positive *S. aureus* (mostly existing on the body surface of mammals), Gram-negative *E. coli* (a widespread intestinal bacteria of mammals), and *P. aeruginosa* by a viable cell-counting method.

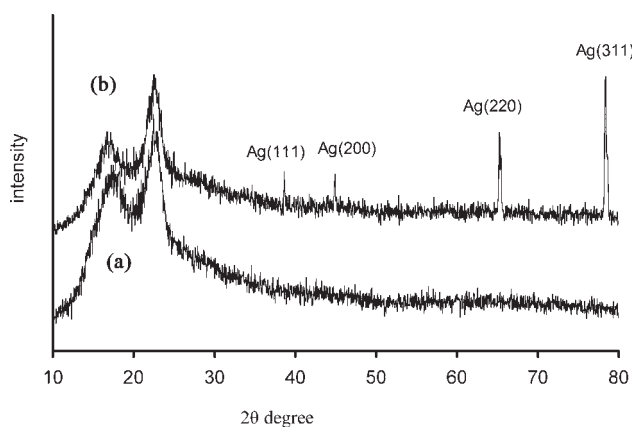


Figure 8 XRD pattern of acrylic nanofibers produced from 13% PAN/DMF solutions (a) without and (b) with 0.5 wt % silver salt.

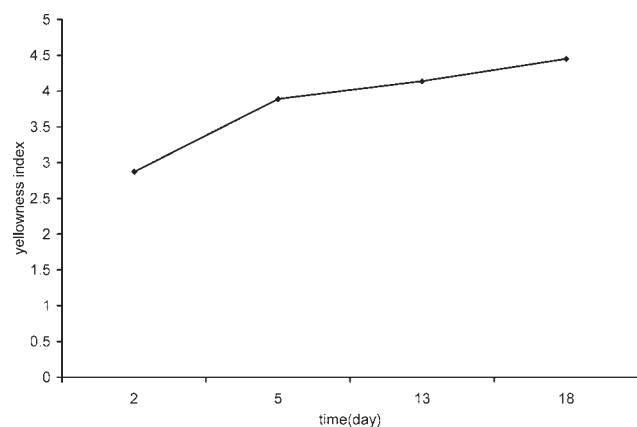


Figure 9 YI versus aging time of a nanofiber web prepared from a 10% PAN/DMF solution containing 0.5 wt % silver salt.

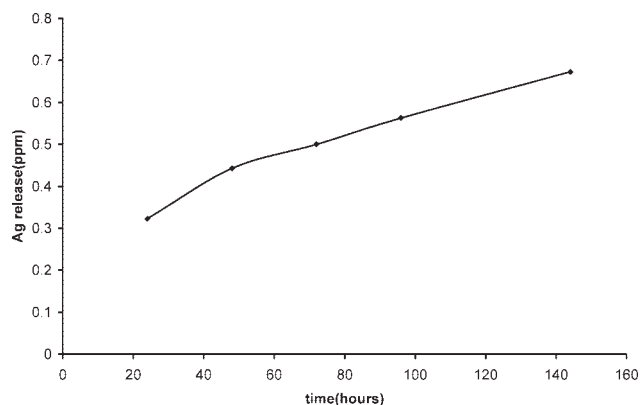


Figure 10 Silver release of a nanofiber web produced from 10% PAN/DMF containing 0.5% silver nitrate.

Gram-negative bacteria are responsible for more than 80% of all infections.³⁰ Tests were carried out six times against each bacterium.

The reductions of bacteria were calculated according to the following equation:

$$\text{Reduction (\%)} = (B - A)/B - 100 \quad (8)$$

where A and B are the surviving cells (cfu/mL) for the plates containing test samples and the control, respectively, after 1 h of contact time.

The results are shown in Table III. Acrylic nanofibers containing silver nanoparticles showed good antibacterial features, especially against *P. aeruginosa*. These nanofibers killed $97.7 \pm 2.95\%$ of *P. aeruginosa*, $54.8 \pm 2.82\%$ of *E. coli*, and $72.9 \pm 3.07\%$ of *S. aureus*.

Figure 11 shows typical plates that contained 10^5 cfu/mL *P. aeruginosa* with the test sample (a sample that contained silver nanoparticles) and a blank sample.

CONCLUSIONS

The results of this research showed that silver nanoparticles can be prepared through the *in situ* reduction of silver ions in a PAN/DMF solution after 4 h of irradiation by a xenon arc without any additional

TABLE III
Results of the Antibacterial Tests for the Acrylic Nanofibers Containing Silver Nanoparticles Against *P. aeruginosa*, *E. coli*, and *S. aureus*

Test number	Reduction (%)		
	<i>P. aeruginosa</i>	<i>E. coli</i>	<i>S. aureus</i>
1	99.9	53.3	75
2	99.9	57.6	75
3	99.9	52.9	68.9
4	99	59	73
5	94	54	76
6	94	52	63.9

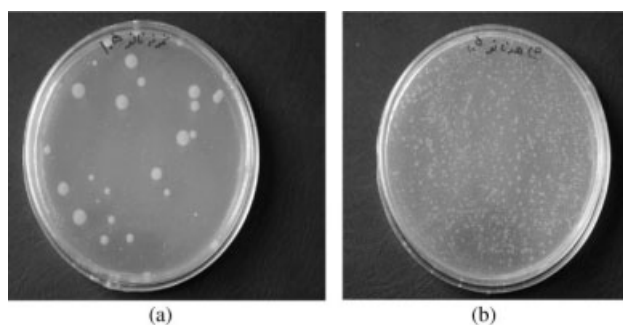


Figure 11 Plates contain 10^5 cfu/mL *P. aeruginosa*: (a) test and (b) blank samples.

chemicals used as reducing agents. UV-vis spectra showed, first, that PAN is a suitable stabilizer for silver nanoparticles and, second, that the size distribution and number of nanoparticles in the colloidal solution can be controlled by the irradiation time interval. TEM images showed that nanoparticles with a mean diameter of about 10 nm were well dispersed in the PAN/DMF solution. SEM images demonstrated that with the addition of up to 0.5 wt % silver salt to the solution, the electrospinning process improved, and the bead number and mean diameter of the nanofibers decreased. According to the FTIR spectra, the nitrile groups in the PAN chains polymerized in the presence of silver ions. The XRD patterns showed that the face-center cubic silver nanoparticles were present in the nanofiber web. Moreover, with the addition of silver salt to the electrospinning solution, the polymer crystallinity increased. The atomic absorption results and antibacterial tests showed that the web of nanofibers had steady and good antibacterial activity, especially against *P. aeruginosa*.

The authors acknowledge the support provided by Isfahan University of Technology, Iranian Nanotechnology Initiative, and Nano Pac Persia Co. and also help given by Mrs. Shafizadegan.

References

- Wang, Y.; Yang, Q.; Shan, G.; Wang, C.; Du, J.; Wang, S.; Li, Y.; Chen, X.; Jing, X.; Wei, Y. *Mater Let* 2005, 59, 3046.
- Yang, Q.; Li, D.; Hong, Y.; Li, Z.; Wang, C.; Qiu, S.; Wei, Y. *Synth Met* 2003, 137, 973.
- Son, W. K.; Youk, J. H.; Lee, T. S.; Park, W. H. *Macromol Rapid Commun* 2004, 25, 1632.
- Lee, H. K.; Jeong, E. H.; Beak, C. K.; Youk, J. H. *Mater Let* 2005, 59, 2977.
- Jin, W. J.; Lee, H. K.; Jeong, E. H.; Park, W. H.; Youk, J. H. *Macromol Rapid Commun* 2005, 26, 1903.
- Xu, X.; Yang, Q.; Wang, Y.; Yu, H.; Chen, X.; Jing, X. *Eur Polym J* 2006, 42, 2081.
- Grafe, T. G.; Graham, K. M. Presented at Fifth International Conference, Nonwovens in the Filtration, Stuggert, Germany, March 2003.

8. Greiner, A.; Wedorff, J. H. *Angew Chem Int Ed* 2007, 46, 5760.
9. Huang, Z. M.; Zhang, Y. Z.; Kotaki, M.; Ramakrishna, S. *Compos Sci Technol* 2003, 63, 2223.
10. Zhang, W.; Qiao, X.; Chen, J. *Mater Sci Eng B* 2007, 142, 1.
11. Hong, K. H. *Polym Eng Sci* 2007, 47, 43.
12. Dwling, D. P.; Betts, A. J.; Pope, C.; Mcconnell, M. L.; Eloy, R.; Arnaud, M. N. *Surf Coat Tech* 2003, 163, 637.
13. Schierholz, J. M.; Lucast, L. J.; Rump, A. *J Hosp Infection* 1998, 40, 257.
14. Samuel, U.; Guggenbichler, J. P. *Int J Antimicrob Ag* 2004, 23, 75.
15. Lala, N. L.; Ramaseshan, R.; Bojun, L.; Sundarrajan, S. *Biotechnol Bioeng* 2007, 97, 1357.
16. Yeo, S. Y.; Lee, H. J.; Jeong, S. H. *J Mater Sci* 2003, 38, 2143.
17. Lee, H. J.; Yeo, S. Y.; Jeong, S. H. *J Mater Sci* 2003, 38, 2199.
18. Patakfalvi, R.; Zsnett, V.; Dekany, I. *Colloid Polym Sci* 2004, 28, 299.
19. Lu, H. W.; Liu, S. H.; Wang, X. L.; Qian, X. F.; Zhu, Z. K. *Mater Chem Phys* 2003, 81, 104.
20. Mayer, A.; Mark, J. E. *Polymer* 2000, 41, 1627.
21. Zhao, X. G.; Shi, J. L.; Hu, B.; Zhang, L. X.; Hua, Z. L. *Mater Let* 2004, 58, 2152.
22. Zhang, Z.; Zhang, L.; Wang, S.; Chen, W.; Lei, Y. *Polymer* 2001, 42, 8315.
23. Yang, X.; Lu, Y. *Mater Let* 2005, 59, 2484.
24. Zhu, Y.; Qian, Y.; Li, X.; Zhang, M. *Nanostruct Mater* 1998, 10, 673.
25. Kim, J. W.; Lee, J. E.; Kim, S. J.; Lee, J. S.; Kim, J.; Han, S. H.; Chang, I. S.; Suh, K. D. *Polymer* 2004, 45, 4741.
26. Shanmugam, S.; Viswanathan, B.; Vardarajan, T. K. *Mater Chem Phys* 2006, 95, 51.
27. Zhu, Y.; Qian, Y.; Li, X.; Zhang, M. *Nanostruct Mater* 1998, 10, 673.
28. Santos, I. P.; Marzan, M. L. *Pure Appl Chem* 2000, 72, 83.
29. Sun, X.; Luo, Y. *Mater Let* 2005, 59, 3022.
30. Xu, X.; Yin, Y.; Ge, X.; Wu, H.; Zhang, Z. *Mater Let* 1998, 37, 354.
31. Jalili, R.; Morshed, M.; Hossaini Ravandi, S. A. *J Appl Polym Sci* 2006, 101, 4350.
32. Mami, T.; Shirai, F.; Makiko, S.; Nanae, I.; Okamoto, Y.; Dohi, Y. *Am J Infect Control* 2004, 32, 27.
33. Abedi, D.; Mortazavi, S. M.; Khajeh Mehrizi, M.; Feiz, M. H. *Text Res J* 2008, 78, 311.
34. Yu, D. G.; Teng, M. Y.; Chou, W. L.; Yang, M. C. *J Membr Sci* 2003, 225, 115.
35. Li, Y.; Leung, P.; Yao, L.; Song, Q.; Newton, E. *J Hosp Infection* 2006, 62, 58.
36. Fritzsche, W.; Porwol, H.; Wiegand, A.; Bornmann, S. *Nanostruct Mater* 1998, 10, 89.
37. Son, W. K.; Youk, J. H.; Park, H. W. *Carbohydr Polym* 2006, 65, 430.
38. Masson, J. C. *Acrylic Fiber Technology and Applications*; Marcel Dekker: New York, 1995; Chapter 8.
39. Amirshahi, S. H. *Basics of Color Technology*; Markaz nashre daneshgahi: Tehran, Iran, 1987; Chapter 5.